Conf-911096--3

Note: This is a preprint of a paper being submitted for publication. Contents of this paper should not be quoted nor referred to without permission of the author(s).

CONF-911096--3

DE92 003512

Invited Plenary paper for the Fourth International Symposium on Superconductivity (ISS '91), October 14–17, 1991, Tokyo, Japan

SUPERCONDUCTING PROPERTIES AND MICROSTRUCTURE OF $YBa_2Cu_3O_{7-\delta}/PrBa_2Cu_3O_{7-\delta}$ SUPERLATTICES

Douglas H. Lowndes,[a] David P. Norton,[a] Shen Zhu,[b] and X. -Y. Zheng [c]

October 1991

[a]Solid State Division
Oak Ridge National Laboratory
[b]Department of Physics and Astronomy, The University of Tennessee, Knoxville, TN
[c]Health and Safety Research Division
Oak Ridge National Laboratory
P. O. Box 2008
Oak Ridge, Tennessee 37831-6056
managed by
MARTIN MARIETTA ENERGY SYSTEMS, INC.
for the
U.S. DEPARTMENT OF ENERGY
under contract DE-AC05-84OR21400

Superconducting Properties and Microstructure of $YBa_2Cu_3O_{7-\delta}$ / $PrBa_2Cu_3O_{7-\delta}$ Superlattices

Douglas H. Lowndes,[a] David P. Norton,[a] Shen Zhu,[b] and X.-Y. Zheng [c], [a] Solid State Division, Oak Ridge National Laboratory, Oak Ridge, TN 37831-6056 USA [b]Department of Physics and Astronomy, The University of Tennessee, Knoxville, TN, [c] Health and Safety Research Division, Oak Ridge National Laboratory, Oak Ridge, TN 37831-6056 USA

ABSTRACT

Epitaxial $YBa_2Cu_3O_{7-\delta}$/$PrBa_2Cu_3O_{7-\delta}$ (YBCO/PBCO) superlattices are tools for systematic, fundamental studies of high-temperature superconductivity. The variation of T_c in YBCO/PBCO superlattices can be understood as arising from changes in the interlayer phase coupling between YBCO layers that are highly two-dimensional when they are very thin (~1–2 *c*-axis unit cells) and completely isolated from each other. Single-cell-thick YBCO layers, containing isolated pairs of CuO_2 planes, are found to be superconducting at $T_c \sim 20$ K, in a PBCO matrix. The resistance in the superconducting transition region scales with temperature as expected for the (flux flow) resistance produced by thermally generated 2D vortices, or for a 2D array of superconducting weak links. Relative to both thin-film and single-crystal HTSc specimens, the thin superconducting layers in YBCO/PBCO superlattices exhibit a greatly expanded temperature range over which characteristic 2D dissipation can be observed, as a consequence of the enhanced anisotropy and reduced dimensionality of the YBCO layers. Scanning tunneling microscope studies reveal that YBCO films and YBCO/PBCO superlattices grow unit cell-by-unit cell by a terraced-island growth mechanism. On miscut, near-(001) substrates the terraces are epitaxially aligned with the substrate crystal lattice and spiral growth structures (screw dislocation-mediated growth) are not seen. These observations explain the steps or "kinks" that are seen in cross-section Z-contrast TEM images of YBCO/PBCO superlattices. The kinks may correspond physically to regions where the supercurrent must tunnel along the *c*-axis, and thus may be weak-link barriers.

KEY WORDS: superlattice, superconductivity, $YBa_2Cu_3O_{7-\delta}$, $PrBa_2Cu_3O_{7-\delta}$, two-dimensional, growth mechanism

INTRODUCTION

For $YBa_2Cu_3O_{7-\delta}$ (YBCO), the zero-temperature *c*-axis superconducting coherence length, $\xi_c(0) \sim 2$–4 Å, [1–3] is comparable to the ~3.9 Å spacing of the two CuO_2 planes within a unit cell and somewhat smaller than the $c \sim 11.7$ Å separation of successive CuO_2 bilayers in adjacent cells. This comparison indicates we should expect strong coupling of the two CuO_2 planes within the YBCO unit cell, as well as significant coupling of CuO_2 bilayers in adjacent *c*-axis unit cells. However, YBCO's effective anisotropy can be greatly increased by artificially separating thin YBCO layers by varying thicknesses of insulating materials, in epitaxial superlattice structures. Consequently, the *c*-axis coupling can be systematically and quasi-continuously varied, and the effect on high-temperature superconductivity studied, including determining the limiting superconducting behavior of isolated, single-cell-thick YBCO layers.

Recent work in several laboratories has demonstrated that high quality high-temperature superconductor (HTSc) superlattices can be fabricated by several different methods [4–12]. Superlattice research using 123-family materials has focused on epitaxial superconductor/insulator structures in which variable-thickness *c*-axis-perpendicular ($c_\perp$) layers of superconducting YBCO alternate with insulating $PrBa_2Cu_3O_{7-\delta}$ (PBCO) [4,6,7,10–12] or its alloys [9]. For example, we have used these YBCO/PBCO structures to show that for a fixed YBCO layer thickness (M = 1, 2, 3,... unit cells), the zero-resistance transition temperature (denoted here by T_c) initially decreases rapidly as the PBCO "barrier" layer thickness is increased, but for a large PBCO layer thickness T_c saturates at a non-zero value that is characteristic of the (fixed) YBCO layer thickness [4,10,11]. In particular, single-cell-thick YBCO layers, containing isolated pairs of CuO_2 planes, were found to be superconducting at $T_c \sim 20$ K in a PBCO matrix [4]. However, the existence of the CuO_2 bilayer structure made it unclear whether the superconductivity of isolated single-cell YBCO layers should be considered two- or three-dimensional (2D or 3D).

Rasolt, Edis, and Tesanovic recently suggested [13] that these YBCO/PBCO superlattices provide a 3D system in which the interlayer (*c*-axis) coupling can be weakened all the way to zero, as indicated by the saturation of T_c values that occurs for large PBCO thicknesses [4]. Thus, a crossover to 2D behavior *must* occur, accompanied by characteristic 2D dissipation [13]. Minnhagen and Olsson also find that the resistive transition data for superlattices containing the thinnest, best-isolated YBCO layers (one or two cells thick) are well explained by the 2D Ginzburg-Landau Coulomb Gas model [14]. Finally, Ariosa and Beck have suggested [15] that each superconducting CuO_2 bilayer in a superlattice structure should be modeled as a 2D array of ultrasmall Josephson junctions. Thus, several recent papers suggest that reduced dimensionality plays an important role in the resistive behavior of these structures.

It is the purpose of this paper to provide a concise summary of analyses and microstructural studies that we and others have carried out recently, in order to test several models that have been proposed for the highly systematic behavior of T_c and of the resistive transitions in YBCO/PBCO superlattices, as functions of the layer thicknesses and separations. Particular emphasis is placed here on exploiting the variable anisotropy and resulting "tunable dimensionality" of superlattice structures, in order to reveal the physical mechanisms responsible for their behavior.

SUPERLATTICE RESISTIVE TRANSITIONS

Figure 1 displays the normalized resistance $R_n(T) = R(T)/R(100\ K)$ for $1\times N$ and $2\times N$ YBCO/PBCO superlattices [4]. The 1×1, 1×2, and 1×4 superlattices have the same average composition as the 2×2, 2×4, and 2×8 structures, respectively, but have very different T_c values and resistive transition shapes. This establishes that the superconducting behavior is that of periodically layered structures, and not simply random alloys of some average composition. Figure 1 also reveals the importance of having YBCO in adjacent c-axis unit cells in order to raise T_c. The other striking feature of Fig. 1 is the broadening of the resistive transition that is so prominent for the thinnest YBCO layers.

Figure 2 (derived from data similar to that in Fig. 1) shows that for a fixed YBCO layer thickness, increasing the PBCO thickness produces an initial rapid decrease of T_c, *followed by saturation of* T_c at a nonzero value for large PBCO thicknesses, for all of the $M\times N$ structures studied [4]. The saturation values are $T_c \sim 19$, 54, 71, 80, or 87 K for structures with well-isolated 1-, 2-, 3-, 4-, or 8-cell-thick YBCO layers, respectively. Thus, although intercell coupling increases T_c, this work clearly shows that *interlayer coupling is not necessary for superconductivity to occur* and that *single-cell-thick YBCO layers are superconducting* in a PBCO matrix [4].

In contrast to the behavior shown in Figs. 1 and 2, Kanai et al. [8] have used $Bi_2Sr_2(Ca_{1-x}Y_x)_1Cu_2O_8$-based superlattices, in which superconducting (x=0.15) and semiconducting (x=0.5) layers alternate, to show that there is almost no change in the midpoint transition temperature ($T_{c(mid)} \sim 65$ K) with decreasing superlattice period. Taken together with our results for YBCO/PBCO superlattices, these results emphasize again that high-T_c superconductivity is an intrinsic property of CuO_2 bilayers, but that 3D interactions are present and significant for 123-family materials.

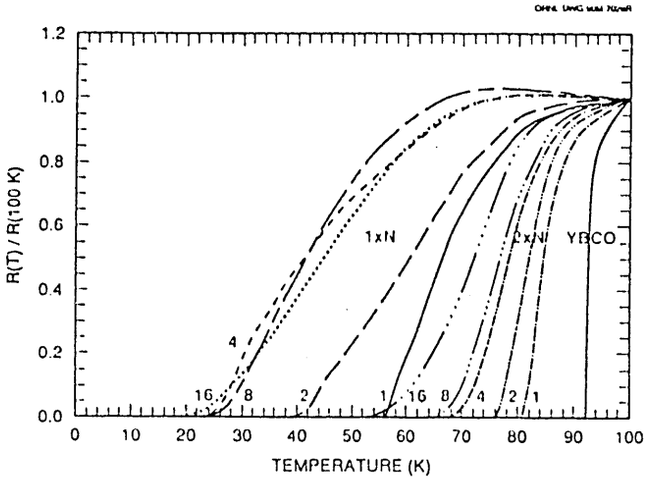

Fig. 1. Normalized resistance vs temperature for $1\times N$ and $2\times N$ superlattices.

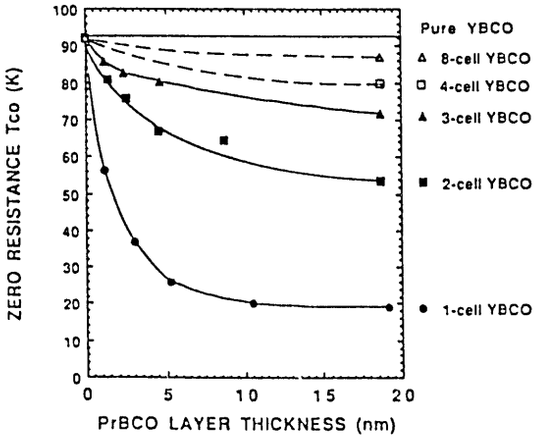

Fig. 2. T_c vs PBCO layer thickness for superlattices with 1- through 8-cell-thick YBCO layers.

EVIDENCE OF CHARACTERISTICALLY 2D DISSIPATION

YBCO/PBCO superlattices provide a 3D system in which the interlayer coupling can be weakened all the way to zero, as evidenced by the saturation of T_c values with increasing PBCO thickness (Fig. 2). Consequently, as Rasolt et al. [13] and Minnhagen and Olsson [14] have pointed out, a crossover to 2D resistive behavior *must* occur for sufficiently thin YBCO layers, as the PBCO thickness is increased. When crossover occurs, characteristic 2D dissipation processes should be observed, specifically resistance in the 2D superconducting state due to free vortices that are produced by thermal unbinding of vortex-antivortex pairs [16–19]. A low temperature Kosterlitz-Thouless (KT) transition also may occur, if a 3D superconducting transition caused by residual interplane coupling does not intervene

first [14] (for intermediate PBCO thicknesses). We emphasize that this is most interesting behavior for crystalline epitaxial specimens, since most previous observations of characteristically 2D dissipation, in non-HTSc materials, have required using granular or amorphous thin films in the dirty limit [20–23].

We define T_{KT} as the *KT* transition temperature, above which thermal unbinding of vortex-antivortex pairs produces free vortices [16,17]. One of the characteristic "signatures" of a 2D conductor is that in the temperature range well below the mean-field (bulk, or BCS) superconducting transition temperature, T_{cB}, but above T_{KT}, the thermally generated vortices produce a nonzero resistivity with temperature dependence [18,19]

$$R(T)/R_N \sim \xi_+(T)^{-2} = \xi_{ab}(T_c)^{-2} \exp[-2b'(\tau_c/\tau)^{1/2}]. \quad (1)$$

In Eq. (1) R_N is the normal-state resistance, $\xi_+(T)$ is the phase correlation length for the superconducting order parameter [18,19], $\xi_{ab}(T)$ is the Ginzburg-Landau correlation length within the *a-b* plane, $\tau_c = (T_{cB} - T_{KT})/T_{KT}$, $\tau = (T - T_{KT})/T_{KT}$, and b' is a constant of order unity. From Eq. (1) it follows that log R(T) should scale as $\tau^{-1/2}$.

Figure 3 shows the result of plotting log $R_n(T)$ vs $\tau^{-1/2}$, where $R_n(T) = R(T)/R(100\ K)$, for the M(YBCO) × 16 (PBCO) superlattice structures [4,10]. These are the structures with the thickest PBCO layers, for which the saturation of T_c suggests that a crossover to 2D resistive behavior is required. Very good agreement with the expected scaling behavior is observed, and from these plots we extract least-squares best-fit values for the *KT* transition temperature of T_{KT} = 14, 44, 70, and 86.5 K, for the structures with 1-, 2-, 3-, and 8-cell-thick YBCO layers, respectively.

Moreover, examination of the resistive behavior of a wide range of other superlattices, for which the barrier layers are not so thick, shows that 2D fluctuations are quite generally important in these structures. For 2- and 3-cell-thick YBCO layers, good straight-line behavior is obtained in plots of log $R_n(T)$ vs $\tau^{-1/2}$, until the PBCO barriers become

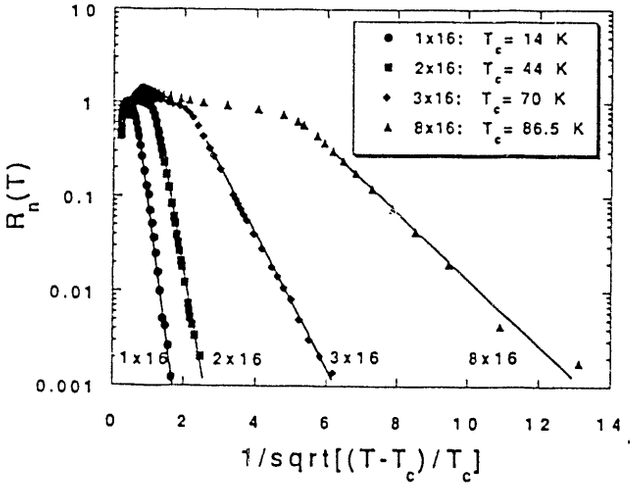

Figure 3. Log $R_n(T)$ vs $\tau^{-1/2}$ for $M \times 16$ superlattices.

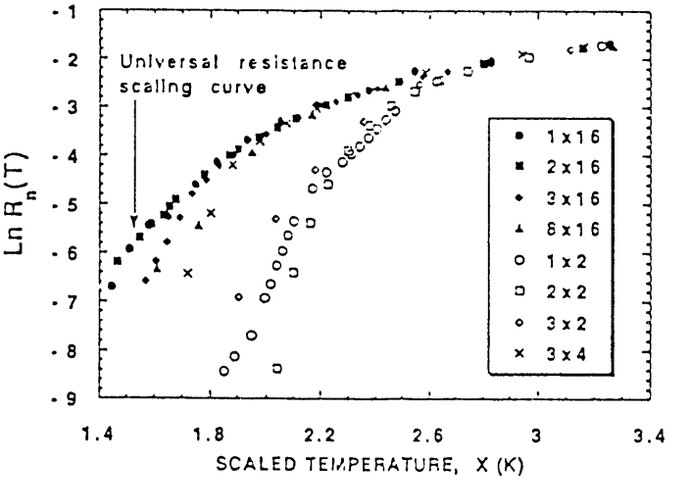

Fig. 4. Logarithm of the normalized resistance vs X(T) for selected YBCO/PBCO superlattices. The X(T) values are calculated from Eq. (3), using fitted values of T_{co} and T_{KT}.

very thin ($N \sim 2$) [4,10]. The best-fit T_{KT} values rise again rapidly toward $T_{cB} \sim 92$ K for a thick YBCO film, either as the YBCO superconducting layers are made thicker or as the PBCO barriers are made thinner, corresponding to a reduced temperature range for 2D behavior, as *c*-axis interlayer coupling is introduced [10].

PURE 2D BEHAVIOR AND 2D–TO–3D CROSSOVER DUE TO INTERLAYER COUPLING

At this point we wish to show the deviations from pure 2D behavior that occur as interlayer coupling is restored between initially isolated YBCO layers (anisotropy reduced). Minnhagen and Olsson have shown how the onset of 3D behavior can be displayed by using the 2D Coulomb gas scaling concept and the 2D Ginzburg-Landau Coulomb Gas (GLCG) model to analyze the superlattice data [14]. The key point, due to Minnhagen [23,24] is that the GLCG model describes the vortex fluctuations in a 2D conductor in terms of a temperature scaling variable, X(T). Consequently, the normalized resistance $R_n(T)$ for all 2D superconductors that are correctly described by the GLCG model should fall on a single, "universal" curve when plotted versus the scaling variable *X* [14,24]. The form of this scaling curve (see Fig. 6) has been well-established from data for type-II superconductor films and also has been related to the GLCG model through Monte Carlo simulations [14].

The scaling variable X(T) is defined by

$$X(T) = [\, T / n^{2D}(T) \,] / [\, T_{KT} / n^{2D}(T_{KT}) \,] , \qquad (2)$$

where n^{2D} is the areal density of supercurrent carriers for the 2D superconductor (not renormalized with respect to vortex fluctuations) [14] and T_{KT} is the Kosterlitz-Thouless transition temperature. Minnhagen and Olsson assume a standard Ginzburg-Landau (GL) description for the temperature-dependence of n^{2D} in the absence of vortex fluctuations, so that $n^{2D}(T) \propto T_{co} - T$, where T_{co} is the GL temperature ($\sim T_{cB}$). Consequently, the scaling variable X(T) becomes

$$X(T) = [\, T / (T_{co} - T) \,] / [\, T_{KT} / (T_{co} - T_{KT}) \,] , \qquad (3)$$

where T_{co} and T_{KT} are used as fitting parameters in the $R_n(T)$ data analysis.

According to Minnhagen and Olsson, T_{co} should be regarded as the temperature at which the superconducting transition would have occurred, if the superconductor was well described by the GL model and there were no vortex fluctuations [14]. T_{KT} is the temperature at which the *KT* phase transition (the onset of vortex-antivortex unbinding) would take place [20, 23]. However, they also point out that layered materials in general (and superlattices in particular) will usually have a 3D phase transition that is caused by residual interplane coupling at a temperature $T_c > T_{KT}$, and that below T_c there is true long-range (3D) order. In summary, T_{co} can be thought of as parameterizing the temperature-dependence of n^{2D}, T_c is the true (experimental) 3D critical temperature, and T_{KT} is the temperature at which the *KT* transition would have occurred (for zero interplane coupling) if 3D ordering had not intervened. Thus, as Minnhagen and Olsson have emphasized, [14] the universal resistance scaling curve (Fig. 4) does not reflect any critical phase transition properties of the vortex fluctuations. It describes only non-critical properties, outside of the *KT* transition region. Nevertheless, T_{KT} and T_{co} can be estimated by fitting the $R_n(T)$ data in this region. The $R_n(T)$ data then can be plotted versus the scaling variable *X*, calculated now from the fitted values of T_{co} and T_{KT}, using Eq. (3).

As shown in Fig. 4, the $R_n(T)$ data for the 1×16 and 2×16 superlattices fall on the 2D scaling curve, indicating that isolated 1-and 2-cell-thick YBCO layers behave as 2D conductors. However, the data for the 3×16 and 8×16 structures deviate from the universal scaling curve, presumably due to coupling between the adjacent YBCO cells in the thicker but still-isolated YBCO layers. Minnhagen and Olsson point out that the close adherence to the universal curve by the data for the thinnest, isolated YBCO layers, can be regarded as confirming that the resistance close to the transition temperature is due to 2D vortex fluctuations, as well as the validity of the 2D GLCG model [14].

On the other hand, we can exploit the variable anisotropy of superlattices to deliberately strengthen the interlayer coupling. Figure 4 also shows data for a series of *M*×2 structures, with only two-cell-thick PBCO barrier layers, for which $R_n(T)$ deviates drastically from the universal scaling curve. Clearly, interlayer coupling through these thin PBCO layers is significant, and all of the YBCO layers in the superlattice must be regarded as being coupled together.

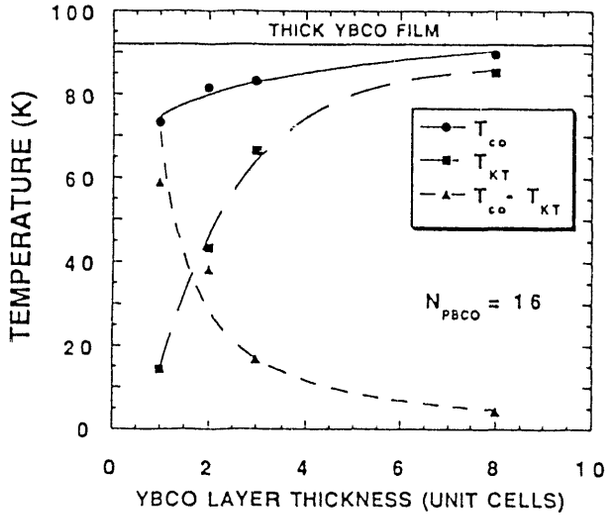

Fig. 5. Transition temperatures and widths vs YBCO layer thickness, for superlattices with well-isolated YBCO layers (N = 16).

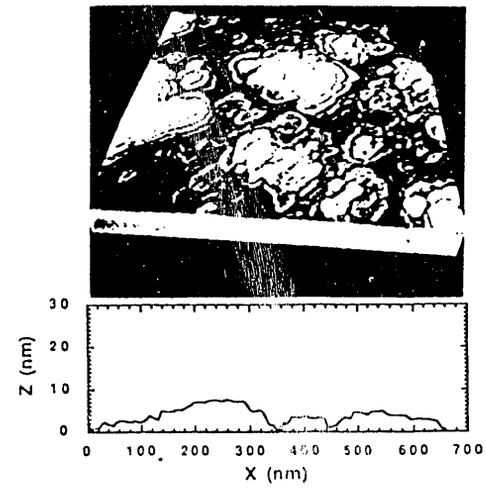

Fig. 6. [Top] STM image of a ~200 nm thick, $c_\perp$ YBCO epitaxial film grown on (001) $SrTiO_3$ at T_{heater} ~730°C. The dimensions of the region shown are 670 × 670 nm^2. [Bottom] Line-scan surface-height profile of the film.

Figure 5 summarizes the effect of 2D excitations in broadening the superconducting transitions of the thinnest YBCO layers. Here we plot the values of T_{KT} (representing the onset temperature for 2D dissipation) and T_{co} (the 3D Ginzburg-Landau temperature) for superlattices with isolated YBCO layers (N = 16 unit cells) of variable thickness (M = 1 to 8). T_{KT} rises rapidly toward a thick YBCO film's T_c ~ 92 K, and the transition broadening, $\Delta T_c = T_c - T_{KT}$, which is so prominent for the thinnest YBCO layers and is due to the 2D excitations, nearly vanishes for a YBCO layer only 8-unit-cells thick. This figure illustrates YBCO's transition from a highly anisotropic 2D conductor to a less anisotropic 3D conductor, over a thickness range of only a few unit cells.

MICROSTRUCTURE AND GROWTH MECHANISM

We recently used scanning tunneling microscopy [25] (STM) and cross-sectional Z-contrast scanning transmission electron microscopy [26] (Z-STEM) to study both near-surface and sub-surface microstructures in "123" films and YBCO/PBCO superlattices. From these studies we were able to determine their growth mechanism.

Our STM images show that $c_\perp$ YBCO films deposited on accurately cut (001) substrates grow by an island growth mechanism. The islands consist of stacks of terraces with step heights that are multiples of the c-axis lattice parameter [25]. Figure 6 shows a STM image of the surface of a $c_\perp$ YBCO film grown at a heater temperature of 730°C on (001) $SrTiO_3$. Well-defined islands are present, each island consisting of a stack of terraces. Variations of this terraced-island morphology are common to all of the $c_\perp$ films that we have studied on a variety of (001) substrates, including $LaAlO_3$, $KTaO_3$, MgO and Y_2O_3-stabilized ZrO_2.

However, we find that the surface microstructure and growth mechanism of YBCO films is extremely sensitive to the substrate miscut angle [27]. In particular, the spiral growth structures [25, 28, 29] that are so prominent (see Fig. 6) in YBCO films grown on accurately-cut (001) substrates, can be completely eliminated by growing YBCO on a substrate that is miscut by only 2 – 3 degrees away from (001). Figure 7 shows the striking effect that substrate miscut angle, θ_m, has in modifying the granularity and growth mechanism of a nominally 16-cell (188 Å) thick YBCO film grown at 720°C on a $LaAlO_3$ substrate with θ_m = 2.7°. The film consists of overlapping tilted platelets; a line scan profile of the surface shows that each platelet is exactly one c-axis unit cell (~ 11.7 Å) thick. The exposed terrace widths of successive platelets are ~30 nm. The tilt angle of the one-cell-thick platelets, determined directly from Fig. 7, is 2.5° (±0.6°), showing that the platelets are epitaxially aligned (within measurement error) with the underlaying $LaAlO_3$ crystal lattice.

There is no sign in Fig 7 of the spiral growth structures that are commonly seen in YBCO films grown on accurately-cut (001) substrates [28, 29]. Instead, another type of terraced, unit cell-by-unit cell growth occurs. The rapid growth direction for YBCO films is perpendicular to the c-axis, i.e., material is most easily added at the rapid-growth a-c and b-c faces of the unit cell. Fig. 7 shows that on a substrate with sufficiently large miscut angle, YBCO apparently takes advantage of the high density of surface steps to nucleate and align the rapid-growth a-c and b-c crystal faces; the platelets then rapidly grow out atop one another in the a-b directions. For θ_m = 2.7°, the average spacing between

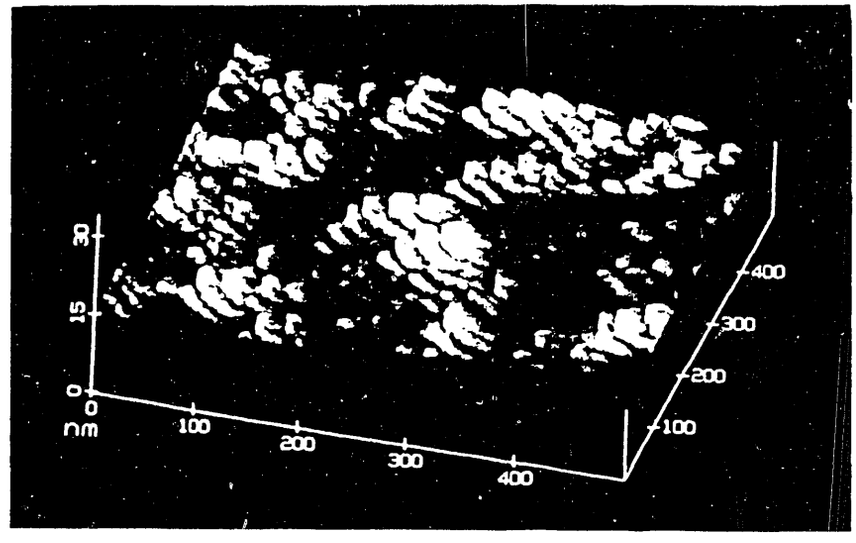

Fig. 7. STM image of surface microstructure of anominally 16-cell-thick YBCO film grown at 720°C on a miscut $LaAlO_3$ substrate with θ_m = 2.7°.

successive 0.39 nm tall $SrTiO_3$ unit cells is ~8.3 nm, corresponding to an average minimum horizontal separation of ~25 nm between successive single-cell-thick YBCO layers. This minimum separation is in good agreement with the

actual ~28 nm widths of the exposed terraces at the early stage of growth shown in Fig. 7. A significantly miscut surface simultaneously exposes a large number of nucleation and rapid-growth sites, from which simultaneous growth of many terraces can occur, closely analogous to the lateral growth that can occur from a stack of upward-spiraling terraces. Thus, both the spiral-mediated and the miscut growth mechanisms result in grains that are stacks of terraces one unit cell in height, and both are rapid-growth mechanisms, in that numerous terrace-edge sites are continuously made available for growth.

The terraced structure in these images clearly shows that YBCO islands grow unit cell-by-unit cell. Terashima et al. [30] also concluded that YBCO films grow unit cell-by-unit cell, based on their observations of RHEED oscillations during YBCO growth on (001) $SrTiO_3$ by reactive evaporation. They used precise x-ray measurements of film thickness to show that each RHEED oscillation corresponded to a layer thickness increment of one *c*-axis lattice constant (~1.17 nm). However, they interpreted the RHEED oscillations as being due to nucleation of 2D islands and to their growth in flat layers in a cyclic fashion. Norton et al. [25] have pointed out that the strictly layer-by-layer description proposed by Terashima et al. is not completely consistent with the granular, variable-height surface that STM reveals for ~200 nm-thick films. The resolution of this apparent difference probably is that Terashima et al. reported RHEED oscillations only during the initial stages of epitaxy, and at a low substrate temperature (~ 680°C). Terashima et al. also have pointed out that unit cell-by-unit cell growth implies that for YBCO the minimum structural unit that can satisfy the requirements of stoichiometry and charge neutrality is the full unit cell [30].

The individual terraces on a particular island/grain are flat on nearly the atomic scale. However, the terraced-island growth mechanism leads naturally to a gradual "roughening" of the growing surface (gentle undulations of surface height or film thickness), as one moves from the center to the edge of an island/grain that has coalesced with an adjacent island/grain. The height variation is a function both of film thickness and substrate temperature. For ~200 nm-thick films, the surface "roughness" is ~10 nm for films grown at a heater temperature of 730°C, and ~30 nm at 780°C [25].

CONSEQUENCES OF MICROSTRUCTURE: WEAK-LINK BEHAVIOR?

The surface microstructures observed by STM for $c_\perp$ YBCO films may have important implications for the transport properties of YBCO/PBCO superlattices, because both the terraced steps and larger-scale undulations on the growing surface should be translated into the individual YBCO layers in a superlattice structure. If we imagine a PBCO layer with terraced steps on it at the time when the laser ablation targets are exchanged in order to grow the next YBCO layer, then it is clear that the individual YBCO layers in superlattices will not be flat but will have steps or "kinks" in them wherever they cross the ends of PBCO terraces: The crystalline continuity of the superlattice is unaffected, but the chemical contents of a particular one-unit-cell crystalline layer will change from Y to Pr. We have observed these steps in the YBCO layers of superlattices, using cross-section Z-STEM [10, 11, 26]. The average lateral distance, L_s, between the steps (or kinks) kinks in cross-section Z-STEM images was $L_s \sim 20$ nm, consistent with the average separation of 15 ± 5 nm between successive terrace steps, observed via STM for films grown at a heater temperature of 730°C.

The STM images also indicate that the individual YBCO layers in superlattices should not be expected to be flat, but will undulate up and down by ~10–30 nm (depending on growth temperature) over lateral distances corresponding to a grain/island diameter (~100–500 nm, also depending on growth temperature); the undulation amplitude is largest for the YBCO layers closest to the film surface. These undulations also can be seen clearly in cross-section Z-STEM images (e.g., Fig. 1 of Ref. 26).

The *c*-axis superconducting coherence length, $\xi_c \sim 2$–4 Å [1–3], is much smaller than $c \sim 11.7$ Å. Consequently, the existence of "kinks" in the chemical continuity of thin YBCO layers means that the supercurrent must tunnel at least one cell along the *c*-direction for every distance L_s that it travels laterally. For single-cell-high kinks in an M-cell-thick YBCO layer, this should have no serious effect on the critical current density, J_c, or transition temperature, T_c, unless $M = 1$ or 2, because the average "overlap" of the two adjacent pieces of the YBCO layer at the kink will be M-1 cells. However, for a 1×N superlattice, the average overlap of the YBCO layer at the kink is zero, and its continuity then depends entirely on there being enough "chance" areas of overlap in different in-plane directions to produce a continuous percolative path, or else on *c*-axis tunneling [26]. Consequently, for 1×N structures, one expects clear weak-link behavior, including a significant reduction of J_c (which we observed [26]) and a depression of T_c (as described above), due to the disruption of the phase of the superconducting order parameter at these weak-link kinks.

Based on these STM observations of surface microstructures of YBCO films, together with Z-STEM images of YBCO/PBCO superlattices, it appears that any theory of superlattice transport properties must include the effects of the

"kinks" in the YBCO layers. A very thin (~ single-cell) YBCO layer probably should be regarded as an array of superconducting regions interconnected by weak-link barriers at the "kinks". Lobb, Abraham, and Tinkham have considered in detail how a vortex-unbinding phase transition would affect various properties of a square lattice of superconducting weak links [31]. They found that the free vortex density is the dominant temperature-dependent factor in the expression for the weak-link array's resistance. Their resulting expressions for the temperature-dependent phase correlation length and resistance are very similar to Eq. (1), except for an additional temperature-dependent factor inside the exponential. This additional factor comes from the temperature-dependent coupling energy, $E_J(T)$, between adjacent superconducting islands [31], which causes the resistance to be expressed in terms of a dimensionless temperature parameter, $k_B T/E_J(T)$. However, Lobb et al. also point out that if $T_c << T_{cB}$ then $E_J(T) \sim E_J(0) \sim$ constant, so that the expressions for $R(T)$ become entirely equivalent for fitting purposes [31].

Thus, the characteristically 2D behavior that we observe in YBCO/PBCO superlattices appears to be entirely consistent both with STM and Z-STEM identification of actual defects in the layers, on the one hand, and with the expected behavior of superconducting layers that are composed of an array of Josephson junctions, on the other. We note that Ariosa and Beck recently suggested that each conducting CuO_2 bilayer in a YBCO/PBCO superlattice should be modeled as a 2D array of ultrasmall in-plane Josephson-coupled junctions [15]. Their model is able to fit the observed variation of T_c with YBCO and PBCO layer thicknesses. However, they did not suggest any particular defect that would correspond physically to the Josephson barrier, nor did they consider the important effect of the barriers on the shape of the resistive transition.

ACKNOWLEDGMENT

This research was sponsored by the Division of Materials Sciences, and by the Superconducting Technology Program for Electric Energy Systems, Advanced Utility Concepts Division, Conservation and Renewable Energy, U.S. Department of Energy under contract DE-AC05-84OR21400 with Martin Marietta Energy Systems, Inc.

REFERENCES

1. A. G. Aronov, S. Hikami, and A. I. Larkin, (1989) *Phys. Rev. Lett.* **62**: 965
2. U. Welp, W. K. Kwok, G. W. Crabtree, K. G. Vandervoort, and J. Z. Liu, (1989) *Phys. Rev. Lett.* **62**: 1908
3. Y. Matsuda, T. Hirai, S. Komiyama, T. Terashima, Y. Bando, K. Iijima, K. Yamamoto, and K. Hirata, (1989) *Phys. Rev. B* **40**: 5176
4. D. H. Lowndes, D. P. Norton, and J. D. Budai, (1990) *Phys. Rev. Lett.* **65**: 1160
5. J.-M. Triscone, M. G. Karkut, L. Antognazza, O. Brunner, and Ø. Fischer, (1989) *Phys. Rev. Lett.* **63**: 1016
6. J.-M. Triscone, Ø. Fischer, O. Brunner, L. Antognazza, A. D. Kent, and M. G. Karkut, (1990) *Phys. Rev. Lett.* **64**: 804
7. Q. Li, X. X. Xi, X. D. Wu, A. Inam, S. Vadlamannati, W. L. McLean, T. Venkatesan, R. Ramesh, D. M. Hwang, J. A. Martinez, and L. Nazar, (1990) *Phys. Rev. Lett.* **64**: 3086
8. M. Kanai, T. Kawai, and S. Kawai, (1990) *Appl. Phys. Lett.* **57**: 198
9. D. P. Norton, D. H. Lowndes, S. J. Pennycook, and J. D. Budai, (1991) *Phys. Rev. Lett.* **67**: 1358
10. D. H. Lowndes and D. P. Norton, "Kosterlitz-Thouless-Like Behavior Over Extended Ranges of Temperature and Layer Thickness in Crystalline $YBa_2Cu_3O_{7-\delta}$/$PrBa_2Cu_3O_{7-\delta}$ Superlattices," 1991 (in press), In: *University of Miami Workshop on Electronic Structure and Mechanisms for High-Temperature Superconductivity*, Plenum Publishing Co.
11. D. H. Lowndes, D. P. Norton, J. D. Budai, D. K. Christen, C. E. Klabunde, R. J. Warmack, and S. J. Pennycook, (1990) In: R. Singh, J. Narayan, and D. T. Shaw, (ed) in *Progress in High-Temperature Superconducting Transistors and Other Devices*, (1990) *SPIE Proceedings* **1394**: 150
12. Ø. Fischer, J. M. Triscone, L. Antognazza, O. Brunner, A. D. Kent, L. Mieville, and M. G. Karkut, (1990) *J. Less Common Metals* **164–165**: 257
13. M. Rasolt, T. Edis, and Z. Tesanovic, (1991) *Phys. Rev. Lett.* **66**: 2927
14. P. Minnhagen and P. Olsson, (1991) *Physical Review Letters* (to be published)
15. D. Ariosa and H. Beck, (1991) *Phys. Rev. B* **43**: 344
16. J. M. Kosterlitz and D. J. Thouless, *J. Phys. C* **6**, 1181 (1972); J. M. Kosterlitz and D. J. Thouless, (1978) *Prog. Low Temp. Phys.* **7**: 373
17. J. M. Kosterlitz, (1974) *J. Phys. C* **7**: 1046.
18. B. I. Halperin and D. R. Nelson, (1979) *J. Low Temp. Phys.* **36**: 599
19. V. Ambegaokar, B. I. Halperin, D. R. Nelson, and E. D. Siggia, (1980) *Phys. Rev. B* **21**: 1806
20. M. R. Beasley, J. E. Mooij, and T. P. Orlando, (1979) *Phys. Rev. Lett.* **42**: 1165
21. J. E. Mooij, (1983) In: B. Deaver and J. Ruvalds (ed) in *Advances in Superconductivity*, Plenum Press, New York, p. 433

22. J. E. Mooij, (1984) In: A. M. Goldman and S. A. Wolf (ed) in *Percolation, Localization, and Superconductivity*, Plenum Press, New York, p. 325
23. P. Minnhagen, (1987) *Rev. Mod. Phys.* **59**: 1001
24. P. Minnhagen, (1981) *Phys. Rev. B* **24**: 6758
25. D. P. Norton, D. H. Lowndes, X. -Y. Zheng, Shen Zhu, and R. J. Warmack, (1 November 1991) *Phys. Rev. B: Rapid Commun.* **44**
26. S. J. Pennycook, M. F. Chisholm, D. E. Jesson, D. P. Norton, D. H. Lowndes, R. Feenstra, and H. R. Kerchner, (1991) *Phys. Rev. Lett.* **67**: 765.
27. D. H. Lowndes, X. -Y. Zheng, Shen Zhu, J. D. Budai, and D. P Norton (in preparation)
28. M. Hawley, I. D. Raistrick, J. G. Beery, and R. J. Houlton, (1991) *Science* **251**: 1587
29. C. Gerber, D. Anselmetti, J. D. Bednorz, J. Mannha.:, and D. G. Scholm, (1991) *Nautre* **350**: 279
30. T. Terashima, Y. Bando, et al., (1990) *Phys. Rev. Lett.* **65**: 2684 .
31. C. J. Lobb, D. W. Abraham, and M. Tinkham, (1983) *Phys. Rev. B* **27**: 150.

END

DATE FILMED

01108192